

THE NATIONAL UNIVERSITY  
of SINGAPORE



School of Computing  
Computing 1, Singapore 117590

**TR20/07**

*Schedulability Analysis of MSC-based System Models*

*Lei JU, Abhik ROYCHOUDHURY  
and Samarjit CHAKRABORTY*

*October 2007*

# Technical Report

## Foreword

*This technical report contains a research paper, development or tutorial article, which has been submitted for publication in a journal or for consideration by the commissioning organization. The report represents the ideas of its author, and should not be taken as the official views of the School or the University. Any discussion of the content of the report should be sent to the author, at the address shown on the cover.*

OOI Beng Chin  
Dean of School

# Schedulability Analysis of MSC-based System Models

Lei Ju      Abhik Roychoudhury      Samarjit Chakraborty  
Department of Computer Science, National University of Singapore  
E-mail: {julei, abhik, samarjit}@comp.nus.edu.sg

## Abstract

Message Sequence Charts (MSCs) are widely used for describing interaction scenarios between the components of a distributed system. Consequently, worst-case response time estimation and schedulability analysis of MSC-based specifications form natural building blocks for designing distributed real-time systems. However, currently there exists a large gap between the timing and quantitative performance analysis techniques that exist in the real-time systems literature, and the modeling/specification techniques that are advocated by the formal methods community. As a result, although a number of schedulability analysis techniques are known for a variety of task graph-based models, it is not clear if they can be used to effectively analyze standard specification formalisms such as MSCs. In this work, we make an attempt to bridge this gap by proposing a schedulability analysis technique for MSC-based system specifications. We show that compared to existing timing analysis techniques for distributed real-time systems, our proposed analysis gives tighter results, which immediately translate to better system design and improved resource dimensioning. We illustrate the details of our analysis using a setup from the automotive electronics domain, which consist of two real-life application programs (that are naturally modeled using MSCs) running on a platform consisting of multiple electronic control units (ECUs) connected via a FlexRay bus.

## 1 Introduction

Message Sequence Charts (MSCs) or Sequence Diagrams are widely used by requirements engineers in the early stages of reactive system design [15, 2, 22]. MSCs can be very convenient for describing communication protocols between a number of agents, e.g., a bus protocol between a bus controller and a number of processing elements trying to negotiate access to the bus. MSCs are therefore a natural choice for modeling and specifying distributed real-time and embedded systems. Consequently, timing and schedulability analysis of MSC-based specifications play an important role in the high-level design of such systems.

However, a significant portion of the work directed towards analysing or reasoning about MSCs and other related specification formalisms focus on functionality validation (such as verification of safety and liveness properties). It is only recently that

quantitative reasoning of such formalisms has attracted a lot of attention [8, 9]. On the other hand, there is a large body of literature on algorithms and techniques for timing and schedulability analysis of real-time systems. However, a large fraction of these techniques are applicable to system models that are essentially based on the concept of *task graphs* [3, 4, 5, 17, 18]. Although such graphs naturally represent data- and control-flow dependencies in periodically or sporadically executing applications [10, 19], they only provide *local* or *processor-centric* views of a distributed system. More specifically, the structuring mechanism used revolves around specifying all the tasks that execute on any given processing (or communication) element. As a result, they are not very suitable for specifying the *interactions* between the multiple entities of a distributed system – which is often a more natural way of specifying such systems.

**Contributions of our work:** In this work we make an attempt to reconcile the above-mentioned gap between the timing/schedulability analysis techniques developed within the real-time systems community and the specification formalisms commonly used for designing large-scale distributed real-time systems. Our main contribution is a schedulability analysis technique for a standard MSC-based system specification of a distributed real-time system. Each MSC in such a specification denotes a *scenario* and captures the partial ordering between various computation and communication tasks/events constituting this scenario. Multiple such MSCs can be combined together to form what is referred to as a **Message Sequence Graph (MSG)** [1, 14], whose edges denote transitions from one scenario to the next. Multiple outgoing edges from a node in such a graph represent conditional transitions, where exactly *one* of the outgoing edges can be activated. A complete system specification consists of a set of such MSGs denoting concurrently running applications that share common resources. Examples of such applications in an automotive electronics setting might be an *adaptive cruise controller*, an *advanced crash preparation system* and a *brake controller* application, all running concurrently and sharing common resources such as electronic control units (ECUs) and communication buses. It may be noted that such a specification is completely standard [22] and is routinely used for modeling and specifying large distributed systems.

In what follows, we use certain standard MSC-specific terminology, which have been explained in Section 2 along with a formal description of MSCs. We extend the system specification described above by mapping the different *lifelines* in a MSC to different processing elements and their associated *messages* to different communication resources (e.g. buses). Further, we annotate the *events* and the *messages* constituting the different lifelines with lower and upper bounds on their execution/communication times. Such execution/communication times do not involve blocking times arising out of resource contentions, which is accounted for by our schedulability analysis. Given this system description, along with the scheduling/arbitration policies at the different resources, our analysis can be used to compute upper bounds on the end-to-end delays associated with various event (and/or message) sequences, which can then be checked against prespecified deadlines. Examples for such sequences might start with data arriving via a sensor, getting processed on several ECUs which also involves multiple transmissions over one or more buses, and then finally ending at an actuator.

There are two standard approaches for schedulability analysis of task graph-based

specifications of real-time systems — worst-case response time analysis-based techniques [6, 13, 16], and the processor demand bound criteria-based analysis [4, 7]. It turns out that neither of these approaches can be applied to our setting in a straightforward manner. This is primarily because in traditional task graph-based specifications, all the vertices are mapped onto a single resource, whereas in our case each MSG (in fact even a vertex of an MSG denoting an MSC) involves multiple computation and communication resources. Hence, the semantics of MSGs are fundamentally different from the task graphs that have been studied in the real-time systems literature.

**Relationship with previous work:** Our proposed analysis is motivated by the response time calculation algorithm presented in [25], which can handle system specifications with multiple computation and communication elements. We have adapted this algorithm to the specific context of MSCs, and in particular proposed two new extensions. (i) The algorithm in [25] is based on a response time analysis framework, which iteratively computes tighter estimates on the response times of various computation and communication tasks. However, it cannot handle conditional transitions which exist in MSGs. We get around this problem by combining the response time analysis-based technique in [25] with a demand bound criteria-based technique that was recently proposed in [3] to handle conditional branches in a different task model. (ii) Compared to [25], we also obtain tighter bounds on the response times of tasks by accounting for the dependencies in the preempting tasks/applications. The main novelty of our work stems from the interesting combination of response time analysis and demand bound criteria-based techniques, which is not commonly seen in the real-time systems literature. This is explained in further detail in Section 2.3 of this report.

Analyzing system specifications with dependencies between computation and communication tasks is known to be a challenging technical problem. This is because the worst-case communication behavior depends on the traffic attempting to access the shared medium, whereas the traffic generated (by the computation inside the tasks) depends on the communication behavior encountered in the past. This naturally leads to an infeasibly expensive analysis which steps through the individual computation and communication steps inside/across tasks. It leads to a further combinatorial blow-up in the presence of conditional transitions. Our proposed analysis – using the combination of response time and demand bound criteria-based techniques – is able to contain this blow-up without leading to overly pessimistic results.

Finally, we would like to point out that there have been a few previous attempts towards developing schedulability analysis techniques for MSC-based system models. However, they either do not fully exploit the event dependencies within an MSC (thereby leading to coarse analysis and pessimistic results, see [23]), or are restricted to the analysis of a single MSC (as opposed to a complete system model with conditional transitions between different scenarios, see [24]).

**Organization of this report:** The rest of the report is organized as follows. In the next section we formally define our MSC-based system models and explain the difficulties involved in analyzing them. In Section 3 we provide an overview of our schedulability analysis technique, followed by the details in Section 4. A detailed case study illustrating the working of our technique is presented in Section 5. Finally, Section 6 outlines some directions for future work.

## 2 Problem Formulation

### 2.1 Message Sequence Graph

Message Sequence Chart (MSC) is widely used in the design of distributed systems and communication protocols. Formally, an MSC is a labeled poset of the form  $Ch = (L, \{E_l\}_{l \in L}, \preceq, \lambda)$  where  $L$  is the set of processes (also called lifelines) appearing in the chart as vertical lines,  $E_l$  is the set of events that the lifeline  $l$  takes part in during the execution of  $Ch$ . The labeling function  $\lambda$  -with a suitable range of labels- describes (a) the messages exchanged by the lifelines and (b) the internal computational steps during the execution of the chart  $Ch$ . Finally,  $\preceq$  is the partial ordering relation over the occurrences of the events in  $\{E_l\}_{l \in L}$ . In particular, the relation  $\preceq$  or  $\preceq^{Ch}$  (we put  $Ch$  as the superscript when necessary to highlight that the partial order belongs to chart  $Ch$ ) is defined as follows.

- (a)  $\preceq_l^{Ch}$  is the linear ordering of events in  $E_l$ , which are ordered top-down along the lifeline  $l$ ,
- (b)  $\preceq_{sm}^{Ch}$  is an ordering on message send/receive events in  $\{E_l\}_{l \in L}$ . If  $e_s$  is a send of message  $m$  by process  $p$  to process  $q$ , and the corresponding receive event is  $e_r$  (the receipt of the same message by process  $q$ ), we have  $e_s \preceq_{sm}^{Ch} e_r$ .
- (c)  $\preceq^{Ch}$  is the transitive closure of  $\preceq_L^{Ch} = \bigcup_{l \in L} \preceq_l$  and  $\preceq_{sm}$ , i.e.  $\preceq^{Ch} = (\preceq_L^{Ch} \cup \preceq_{sm}^{Ch})^*$ .

The preceding definition of MSC is an abstract one, and does not clarify the events appearing in an MSC. The complete MSC language [15] includes several types of events: message sends and receives, local actions, lost and found messages, instance creation and termination etc. However, for simplicity of exposition, we assume that the events inside an MSC is of one of the following forms — *sends, receives and local events*. A local event can denote any terminating computation within a process, i.e., a terminating sequential program.

An MSC only denotes a single scenario in a system execution, which does not form a complete system description. The purpose of the Message Sequence Graph (MSG) is to describe the relation between the basic MSCs by keeping track of the control-flow in the graphical view. Each node in an MSG is a basic MSC. We also define two special nodes  $\nabla$  and  $\Delta$  which denotes the unique start and end state respectively for each MSG. The edges represent the natural operation of chart concatenation. We consider the so-called “synchronous” concatenation where for a concatenation of two charts  $Ch \circ Ch'$  — all events in  $Ch'$  start only after chart  $Ch$  is finished. Two outgoing edges from a single node represent non-deterministic choice, so that exact one of the two successor charts will be executed in each execution. Finally, a execution trace can be defined to be the path from the initial state ( $\nabla$ ) to the final state ( $\Delta$ ) in the MSG and concatenates the sequence of MSCs encountered on the way. Example MSGs are shown in Figure 2 and will be discussed in next section.

In the following we consider acyclic MSGs where there are no loops between initial state ( $\nabla$ ) to the final state ( $\Delta$ ). Of course, there is an outer loop from final state ( $\Delta$ ) to initial state ( $\nabla$ ) denoting periodic behavior repeated forever. We can also extend our

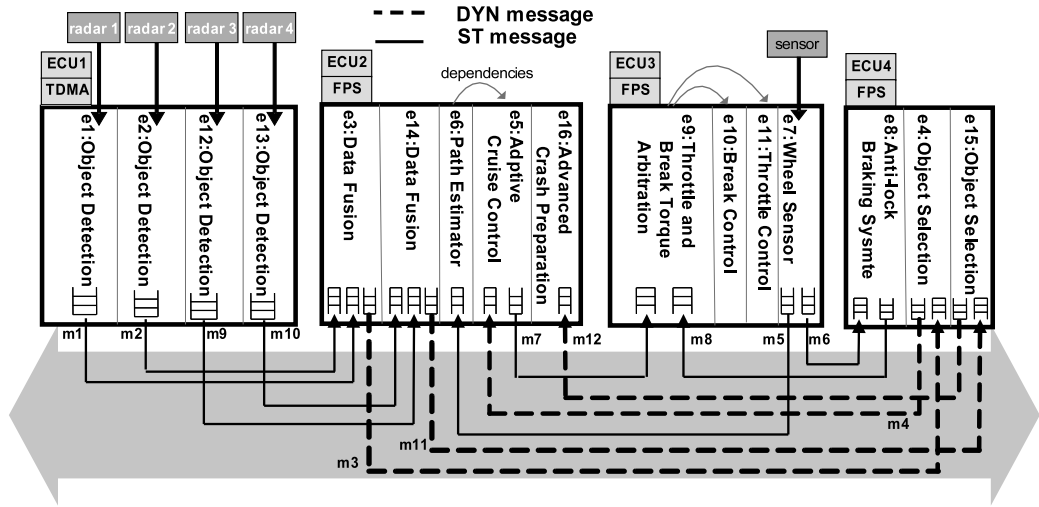


Figure 1: A FlexRay-based ECU network

analysis to allow arbitrary loops in between the initial state ( $\nabla$ ) to the final state ( $\triangle$ ), provided these (inner) loops are bounded.

## 2.2 Running Example

A distributed system has a number of processing elements (PEs) which are connected by shared buses. A typical distributed application consists of a collection of local computations that run on different PEs and communicate with each other through message exchanging via buses. As an example, Figure 1 shows a distributed FlexRay ([11]) based Electronic control unit (ECU) network from the automotive electronics domain. There are four PEs (ECUs) and one shared FlexRay bus in the system. Two concurrently running applications, an Adaptive Cruise Controller (ACC) and an Advanced Crash Preparation (ACP) system, are shown in the example. The ACC application contains local computations  $e1$  to  $e11$  and messages  $m1$  to  $m8$ , while the rest belong to the ACP system. Dependency relations between local computations on the same ECU are also shown, e.g.,  $e10$  and  $e11$  can start only after  $e9$  finishes execution.

Figure 2 shows the MSG models of the ACC and ACP applications in above-mentioned system. As one can see, such applications can be naturally modeled using an MSG model. Each local computation is mapped to a local event on a lifeline in a basic MSC. Note that a lifeline (process) can represent a piece of software program which handles its corresponding event(s), or a hardware functional unit. Thus, the mapping of events onto processes can be easily obtained from the given system specification. According to the resource allocation schema, several processes can share a single PE, which implements its own scheduling policy (e.g. the fix priority preemptive scheduling for processes  $P5$ ,  $P7$ , and  $P8$  on ECU3). It may be noted here that our analysis is flexible enough to handle different scheduling policies, specified both at the MSG, and at the PE/bus level. In fact, the example shown in Figure 1 has a TDMA implemented on ECU1, fixed-priority scheduling implemented on the remaining ECUs

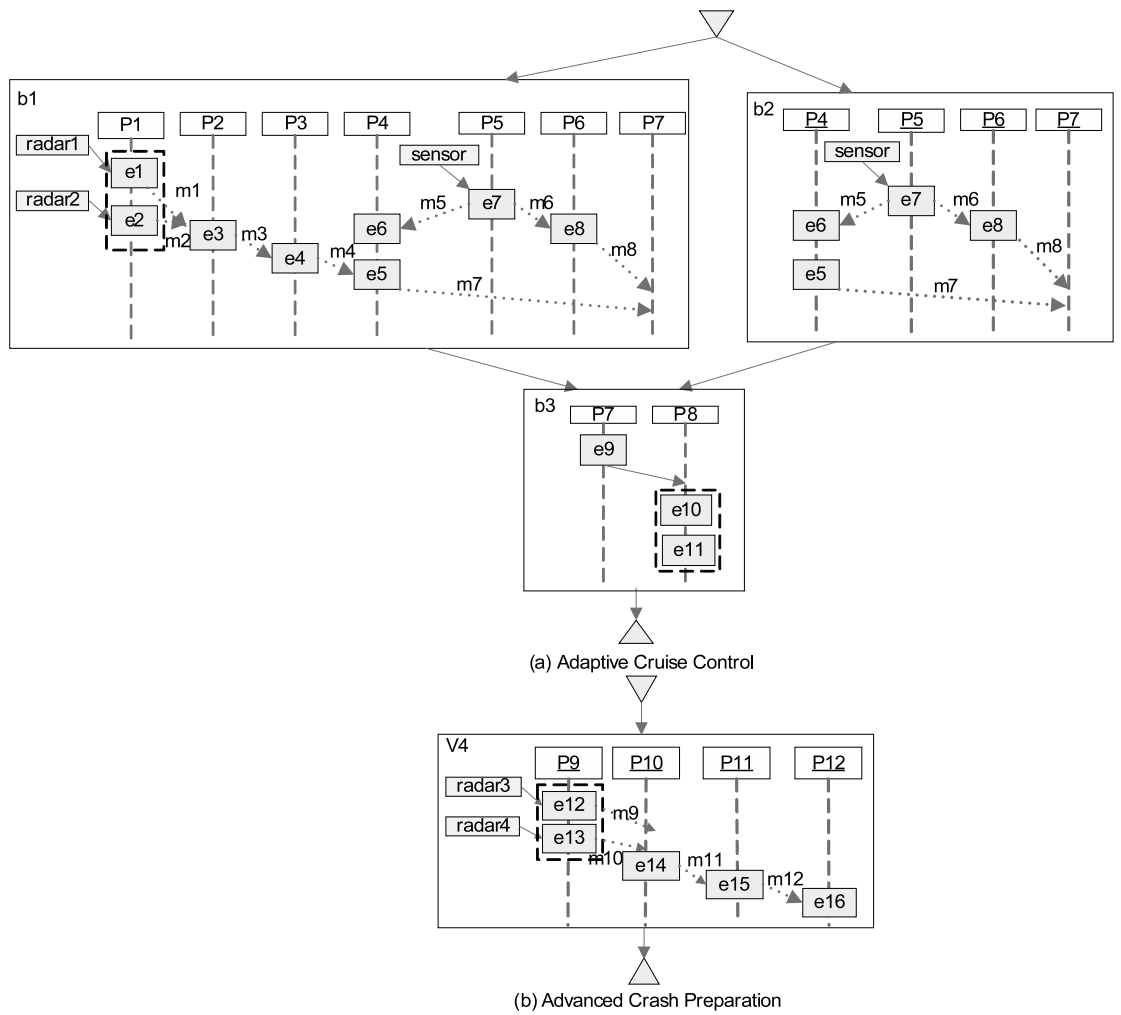


Figure 2: MSG model of the ACC and ACP applications

and a FlexRay protocol implemented on the bus. A communication between two local computations is modeled using a message passing between two processes in a MSC. If the communication is taken via a shared bus, the message name is also shown in the MSC (e.g.,  $m1$  and  $m2$  in MSC  $b1$ ). Since most bus-based communications are asynchronous, we will only consider asynchronous message passing in our MSG modeling. Finally, the data/control dependencies between local computations are reflected by the partial order relation defined within an MSC, as well as the concatenation operations between different MSCs. A coregion (denoted by a dashed-line box) is used to relax the strict ordering of local events along a lifeline, e.g. events  $e10$  and  $e11$  on process  $P8$  of MSC  $b3$  can be executed in any order (depending on the actually scheduling policy of  $ECU3$ )

In our example, the ACC application has three external triggers, namely radar1, radar2 and sensor. We assume the sensor receives input from environment twice faster than the two radars. Consequently, in the start-up stage of a complete run of the ACC application, either it receives input data from both two radars and the sensor, which corresponding to the scenario described as in MSC  $b1$ ; or it receives only the sensor's input which triggers the scenario in MSC  $b2$ , and uses the old output value from the "object selection" ( $e4$ ). The different system behaviors due to environment input are modeled using the indeterministic choice operation from the start of the application.

Given the system architecture and MSG-based modeling of applications, our goal is to perform schedulability analysis by checking whether the worst-case response time (WCRT) for each application meets its deadline. We assume all applications are periodic and independent from each other. In order to perform schedulability analysis, We need to extend the standard MSG formalism with real-time annotations. Each MSG depicting an application is associated with the application's activation period  $P$  and deadline  $D$ . Each event is associated with the best-case and worst-case execution time (BCET/WCET) of its corresponding local computation. We assume the intra-processor communication (e.g., from  $e9$  to  $e10$  and  $e11$  in MSC  $b3$  of Figure 2(a)), as well as the local events of sending/receiving a message (denoted by the start/end of a message arrow), take zero time. Messages are labeled with their transmission time, while the actual communication time (including blocking time due to possible bus contentions) will be calculated by our analysis. Finally, we assume the MSCs are concatenated synchronously.

### 2.3 Issues in Analyzing the Model

Before proceeding to present our schedulability analysis method, let us examine the inherent difficulties in finding end-to-end delay of such an MSG model of distributed application. In order to obtain an accurate analysis for the above-mentioned model, we need to consider the following three factors.

- Contention: Execution of an event may be interfered by other events (from the same application as well as other applications) mapped to same PE, depending on the the scheduling policy of the PE.
- Data/control dependencies: An event (MSC) can be only ready after its predecessor event (MSC) completes.

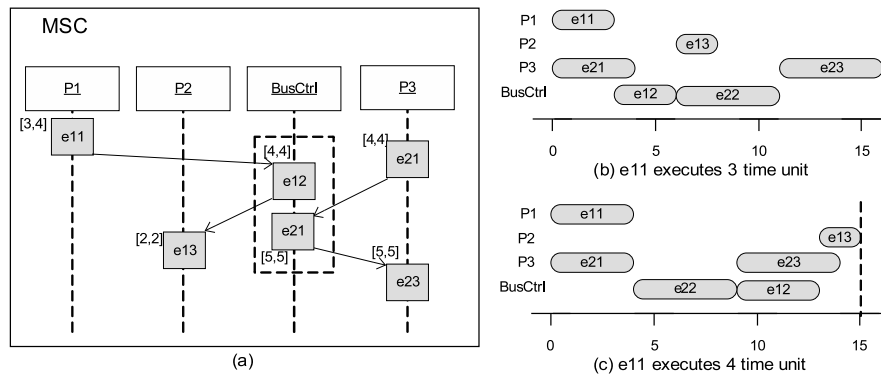


Figure 3: Example of timing anomaly.

- **Conditional Execution:** The execution of an event in the application may depend on some conditions which are (directly or indirectly) set by the environment.

The possible contentions and data dependencies bring the *timing anomaly* phenomenon ([12]) when the execution times of events are non-constant (varying between BECT and WCET). In such case, the local WCET of an event may not lead to the global worst case end-to-end delay of the application. Thus, the worst-case delay of an application cannot be simply obtained by simulating the system using WCET of each individual events, over the LCM of all applications' periods. Figure 3 shows an example of timing anomaly in an MSC-based model. Suppose each process is mapped to a distinct PE connecting via a shared bus, and the bus transaction  $e22$  has a higher priority than the transaction  $e12$ . When the local computation event  $e11$  takes 3 time units to execute, the end-to-end delay for this MSC will be 16, as shown in scenario of Fig. ??(b). However, if  $e11$ 's execution time increases ( to 4 time units), the delay will become smaller (15 time units as shown in Fig. ??(c)).

Existing works on schedulability analysis of MSC-modeled distributed system (e.g. [24] and [23]) compute the local worst-case response time for each individual event in critical instance, which assumes all events are independent. The global worst-case delay is then obtained by summing up these local worst-case response times. However, the dependencies between set of preempting events and preempted events restrict the possible preemption scenarios, which results in the critical/optimal instance assumed for worst/best case response time analysis for set of independent tasks to be too pessimistic/optimistic. For example, suppose events  $e_i$  and  $e_j$  belong to different applications in a system, and they are mapped to the same PE where  $e_i$  has a higher priority than  $e_j$ . If  $e_i$  and  $e_j$  are ready at the same time (thus  $e_i$  imposes the maximum interference on the response time of  $e_j$ ), we could have the following.

- **Dependency between preempting events:** the successor of  $e_i$  (say  $e_k$ ) can not be ready at the same time as  $e_j$ , resulting in  $e_k$  preempting  $e_j$  fewer number of times than it could have preempted in the worst case scenario (where  $e_k$  is ready at the same time as  $e_j$ ).
- **Dependency between preempted events:** subsequent releases of  $e_i$  may not be

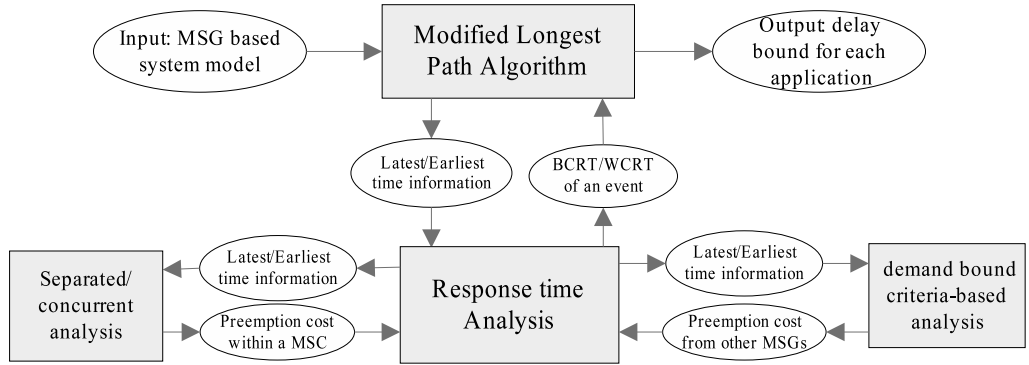


Figure 4: Overview of our analysis framework

ready at the same time as the successor of  $e_j$  (say  $e_p$ ) which also mapped on the same PE, results in less number of preemptions from  $e_i$  on  $e_p$ .

[25] proposes a schedulability analysis based on task (precedence) graph model, which captures the dependency between preempted tasks by capturing phase adjustment between a preempting task and preempted tasks. To retain a conservative analysis, the distance between two preempted tasks must be relatively small to preserve phase adjustment. However, in a bus-based distributed application, it is common to have computations mapped to other PEs as well as bus communications between two preempted events (e.g.  $e_j$  and  $e_p$  in the above-mentioned example). Such gaps in many cases counteract the usefulness of the phase adjustment. On other hand, we adopt the analysis framework from [25] and take into account of the dependency as well as the path information (conditional branching among MSCs) between preempting events for an accurate calculation of best/worst response times and end-to-end delay.

### 3 Analysis Overview

Figure 4 shows the overview our feasibility analysis framework for MSG-based system models. Given a set of MSGs each representing a real-time distributed application and annotated with required timing information, our analysis will return an upper bound on the end-to-end delay for each MSG. We present our analysis method in two levels. In this section, we present the top-level algorithm for analyzing a set of distributed real-time applications modeled using a modified longest path algorithm, which is adopted from [25] with necessary modifications to handle synchronized concatenation and conditional branching for MSG model. In the next section, we will present the WCRT/BCRT calculation of the MSC events.

To facilitate the analysis, four time instances are defined for each event  $e$  and MSC  $M$  in a MSG.

- earliest ready time ( $earliest[e^r], earliest[M^r]$ )
- latest ready time ( $latest[e^r], latest[M^r]$ )
- earliest finish time ( $earliest[e^f], earliest[M^f]$ ), and
- latest finish time ( $latest[e^f], latest[M^f]$ ).

```

1  step = 0; /*number of iteration*/
2  for (each application  $A_i$ ) /*initialization*/
3    latest[ $\nabla_i^t$ ] = earliest[ $\nabla_i^t$ ] = 0;
4  do { /*fix-point iteration*/
5    for (each application  $A_i$ ) {
6      for (each MSC  $M_j$  of  $A_i$  in topologically sorted order) {
7        LatestTimes( $M_j$ );
8        EarliestTimes( $M_j$ );
9        latest[ $M_j^f$ ] =  $\max_{e \in M_j} \{latest[e^f]\}$ ;
10       earliest[ $M_j^f$ ] =  $\max_{e \in M_j} \{earliest[e^f]\}$ ;
11       for (each successor MSC  $M_k$  of  $M_j$ ) {
12         latest[ $M_k^f$ ] =  $\max(latest[M_j^f], latest[M_k^f])$ ;
13         earliest[ $M_k^f$ ] =  $\min(earliest[M_j^f], earliest[M_k^f])$ ;
14       }
15       /*worst case delay of  $A_i$ */
16       wcrct[ $A_i$ ] = latest[ $\Delta_i^f$ ];
17     }
18   }
19   step++;
20 } while (any time instance changed and  $step < limit$ );

```

Figure 5: Delay estimation algorithm.

```

1  LatestTimes(MSC) {
2    /*compute latest[ $e_i^f$ ] and latest[ $e_i^f$ ] for all  $e_i$  in MSC*/
3    for (each source event  $e_i$  in MSC) /*initialize*/
4      latest[ $e_i^f$ ] = latest[MSCr];
5    for (each event  $e_i$  respecting the partial order  $\preceq^{MSC}$ ) {
6       $w_i = WCRCT$  of  $e_i$  /* See Section 4 for details */
7      latest[ $e_i^f$ ] = latest[ $e_i^r$ ] +  $w_i$ ;
8      for (each immediate successor  $e_k$  of  $e_i$ ) {
9        if (latest[ $e_k^r$ ] < latest[ $e_i^f$ ])
10         latest[ $e_k^r$ ] = latest[ $e_i^f$ ];
11      }
12    }
13  }
14 }

```

Figure 6: The LatestTimes algorithm.

Figure 5 presents the top-level iterative algorithm for computing worst case end-to-end delay ( $wcrct[A_i]$ ) for each application  $A_i$ . The top-level analysis uses information of individual events' response times to generate latest and earliest time instances, which in turn will be used to refine the results of response time analysis in the next iteration. The algorithm terminates when (a) no time instance for any of the events is changed (the fixed point is reached), or (b) the maximum number of iteration steps are executed. The top level framework captures the dependencies between individual MSCs. Note that since only one of the conditional edges are taken for each branch, the earliest ready time of a node is set to be the minimum value of the earliest finish times of its predecessors, while the latest ready time of a node is set to be the maximum of the latest finish times of predecessors. The algorithm begins with a very coarse approximation for the start and completion times of the events, and the worst/best case delay it may suffer. The results are refined in each iteration based on the information computed in last iteration. The algorithm is safe in the sense that it never produces under-estimation for the worst case delays or over-estimation for the best case. Thus, our analysis returns a sufficient condition for an application  $A_i$  to be schedulable, if  $wcrct[A_i] \leq D_i$ .

The LatestTimes calculation, shown in Figure 6, is similar to the LatestTimes algorithm in [25]. Basically, the algorithm in Figure 6 uses a modified longest-path

algorithm to take into account data dependencies within a single MSC. Based on dependencies between events of the MSC being analyzed, the main purpose of the algorithm is to update the latest ready and finish times for each event. This updating is independent of the resource scheduling policies on the Processing Elements (PEs). The scheduling policy is only taken into account in the calculation of the worst case response time (WCRT) of an event; this calculation is elaborated in the next section.

Given the `LatestTimes` algorithm, we can easily transform it in to the `EarliestTimes` algorithm, which updates the earliest ready and finish times by calculating the best-case response time for each event.

## 4 Response Time Calculation

The procedure for computing the earliest/latest ready and finish times of MSC events, as discussed so far, only provides an algorithmic framework. In particular, it depends on Worst-case and best-case response time (WCRT/BCRT) estimates of individual events inside the MSCs. We now elaborate the WCRT/BCRT calculation of MSC events. Clearly, this will require us to consider the scheduling policy inside the processing elements on which these events are executed. We assume fixed priority preemptive scheduling for our response time calculation.

The well-known Worst Case Response Time (WCRT) calculation for fixed-priority scheduling of independent periodic tasks is given by the following recursive equation.

$$w_i^{n+1} = c_i + \sum_{t_j \in hp(t_i)} c_j \cdot \lceil \frac{w_i^n}{P_j} \rceil \quad (1)$$

Here  $w_i$ ,  $c_i$ , and  $P_i$  are the response time, computation time, and period for task  $t_i$  respectively. The set  $hp(t_i)$  denotes the set of higher priority tasks mapped to the same PE as  $t_i$ . The fixed point computation starts with  $w_i^0 = c_i$ , and terminates when the response time calculated in  $n + 1$ th iteration ( $w_i^{n+1}$ ) equals to the value in previous iteration ( $w_i^n$ ). Equation 1 computes the WCRT of a task  $t_i$  in its *critical time instance* (i.e. all higher priority tasks are ready when  $t_i$  is ready).

The BCRT calculation is proposed in [21] as

$$b_i^{n+1} = c_i + \sum_{t_j \in hp(t_i)} c_j \cdot (\lceil \frac{b_i^n}{P_j} \rceil - 1) \quad (2)$$

for the same setting. It is based on the best case phasing (or optimal instance) where  $t_i$  finishes simultaneously with the release of all its higher priority tasks.

However, in our distributed MSC-based system model, we can obtain far more accurate WCRT/BCRT estimates by taking into consideration the dependencies between preempting events as discussed in Section 2.3. We divide the worst and best preemption cost on the execution of any event  $e_i$  as follows — (a) preemption on  $e_i$  by other events in the same application (denoted as  $WS_i$  and  $BS_i$ ), and (b) preemption on  $e_i$  by events from other applications (denoted as  $WD_i$  and  $BD_i$ ), respectively. Thus, our WCRT and BCRT equations are given as follows.

$$w_i^{n+1} = c_i + WS_i^n + WD_i^n \quad (3)$$

$$b_i^{n+1} = c_i + BS_i^n + BD_i^n \quad (4)$$

We now elaborate the calculation of these four quantities —  $WS_i, BS_i, WD_i, BD_i$ .

#### 4.1 Preemption within an MSC

Equation 1 and 2 assume deadline less than or equal to period for all tasks ( $D \leq P$ ). This guarantees that, for a schedulable task set, a task instance will not get delayed by any its previous instances. In our analysis, we also make such assumption that deadline is less than or equal to period for all the applications being analyzed. Thus, to show that application  $A$  is schedulable ( $wcrt(A) \leq D$ ), interference from events in previous instances of  $A$  need not to be considered for the critical and optimal time instances. Suppose  $e_i$  and  $e_j$  are events in the same application  $A$ , and there is no dependency between them (neither  $e_i \preceq e_j$  nor  $e_j \preceq e_i$ ). For  $e_j$  to possibly preempt  $e_i$ , the events  $e_i, e_j$  cannot be events in different MSCs of the MSG corresponding to application  $A$ . This is because in any execution of  $A$ , exactly one of the traces represented by the MSG will be executed, and the MSCs along the trace are synchronously concatenated. Moreover,  $e_j$  may preempt  $e_i$  at most once owing to the deadline assumption above.

Furthermore, for  $e_j$  to preempt  $e_i$  in the same MSC  $M$ , there must be overlap between their execution intervals. Let event  $NCP(i, j)$  be the nearest common predecessor event for  $e_i$  and  $e_j$  in  $M$ . If such predecessor event does not exist, we set  $NCP(i, j)$  to be the start of  $M$ . Using the notion of NCP, we define the following quantities.

- smallest time interval between  $NCP(i, j)$  finishing and  $e_i$  becoming ready

$$SFR_i^{NCP(i,j)} = \text{earliest}[e_i^r] - \text{earliest}[NCP(i, j)^f]$$

which corresponds to the scenario that all events on path from  $NCP(i, j)$  to  $e_i$  execute in their BCRT.

- largest time interval between  $NCP(i, j)$  finishing and  $e_i$  becoming ready

$$LFR_i^{NCP(i,j)} = \text{latest}[e_i^r] - \text{latest}[NCP(i, j)^f]$$

which corresponds to the scenario that all events on path from  $NCP(i, j)$  to  $e_i$  execute in their WCRT.

- smallest time interval between  $NCP(i, j)$  finishing and  $e_i$  finishing,

$$SFF_i^{NCP(i,j)} = \text{earliest}[e_i^f] - \text{earliest}[NCP(i, j)^f]$$

- largest time interval between  $NCP(i, j)$  finishing and  $e_i$  finishing,

$$LFF_i^{NCP(i,j)} = \text{latest}[e_i^f] - \text{latest}[NCP(i, j)^f]$$

Executions of two events  $e_i$  and  $e_j$  from the same vertex are guaranteed to be separated in one execution of the MSG if and only if

$$\begin{aligned} separated(i, j) = & e_i \preceq e_j \vee e_j \preceq e_i \vee \\ & (LFF_i^{NCP(i,j)} \leq SFR_j^{NCP(i,j)}) \vee \\ & (LFF_j^{NCP(i,j)} \leq SFR_i^{NCP(i,j)}) \end{aligned}$$

evaluates to true, i.e. either there is a dependency between  $e_i$  and  $e_j$  (as per the partial order for the MSC), or  $e_i$  always finishes before  $e_j$  releases, or vice versa. Note that the instances of  $e_i$  and  $e_j$  involving in the preemption belong to the same run of the MSG. Thus, the above intervals should be measured respected to their nearest common predecessor event (instead of start of the MSG  $\nabla$ ), which gives a much more accurate estimation.

Finally, the worst case preemption cost imposed on event  $e_i$  by events from same application can be calculated as follows: let  $c_j^u$  be the WCET estimate of event  $e_j$ .

$$WS_i = \sum \{ c_j^u \mid contend(j, i) \wedge \neg separated(i, j) \}$$

where  $contend(j, i)$  is true if and only if the events  $e_j$  and  $e_i$  are mapped to the same processing element and  $e_j$  has higher priority than  $e_i$  (as per the scheduling policy of the processing element).

For the BCRT calculation of  $e_i$ , we find the events  $e_j$  that are guaranteed to be ready during  $e_i$ 's execution.

$$\begin{aligned} concurrent(i, j) = & \neg(e_i \preceq e_j) \wedge \neg(e_j \preceq e_i) \wedge \\ & (LFR_i^{NCP(i,j)} \leq SFR_j^{NCP(i,j)}) \wedge \\ & (LFR_j^{NCP(i,j)} \leq SFR_i^{NCP(i,j)}) \end{aligned}$$

The best case preemption cost imposed on event  $e_i$  by events from same application can be calculated as follows: let  $c_j^l$  be the BCET estimate for event  $e_j$ .

$$BS_i = \sum \{ c_j^l \mid contend(j, i) \wedge concurrent(i, j) \}$$

## 4.2 Preemption by a Single MSC

Before computing the preemption cost between full-fledged applications modeled in MSGs, let's first consider the scenario when an event  $e_1$  in application  $A_1$  get preempted by a single MSC  $MSC_2$  in another independent application  $A_2$ .

Figure 7 gives the projection of the events in  $MSC_2$  executed by the same PE as  $e_1$ , including dependencies and priority assignments for the fixed-priority preemptive scheduling on PE. The directed edges in Figure 7 denote event dependencies. Thus, a directed edge from event  $e_i$  to event  $e_j$  indicates  $e_i \preceq e_j$ , as per the partial order  $\preceq$  of the MSC in which  $e_i, e_j$  reside. Note that there might be events in between  $e_i$  and  $e_j$ , which are executed on other PEs. Assume that the set of events within a MSC  $M$  that can preempt an event  $e_i$  is denoted as  $ps_{e_i}^M$ . For instance, in the example given in Figure 7 we have  $ps_{e_1}^{MSC_1} = \{e_2, e_3, e_4\}$ .

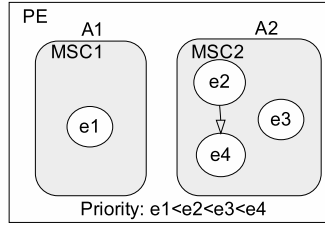


Figure 7: Projection of Events on same PE.

Our goal is to find the worst-case preemption scenario for  $e_i$ , when  $e_i$  is preempted by events in  $ps_{e_i}^M$ . Existing works calculate the WCRT of  $e_i$  by assuming that all events in  $ps_{e_i}^M$  release at the critical instance as  $e_i$  is ready (see equation 1). Clearly, the critical instance assumption will introduce over-estimation on the WCRT of  $e_i$  when dependencies exist between preempting events. In our example,  $e4$  can only be ready some time after  $e2$  finishes. Thus, if  $e2$  is released at the critical time instance (when  $e1$  releases), the worst case number of times  $e4$  can preempt  $e1$  may become less compared to the number assumed in equation 1. In our proposed analysis, we will use the latest / earliest ready and finish times of each event in  $ps_{e_i}^M$ , calculated in each iteration of the delay estimation algorithm shown in Figure 5, to tighten the worst-case preemption cost on  $e_i$ .

Preempting events in  $ps_{e_i}^M$  may either have dependencies (e.g.  $e2$  and  $e4$ ) or execute concurrently with other events (e.g.  $e3$ ). In order to explore number of preemptions they may impose on a particular preempted event, we first construct a *preemption chain* to capture the possible release times of events in  $ps_{e_i}^M$ . A *preemption chain*  $PC_{e_i}^M = \{\hat{N}, \hat{E}\}$ , is a sequence of nodes  $n \in \hat{N}$ , and each directed edge  $E(n_1, n_2) \in \hat{E}$  is labeled with weight  $W(n_1, n_2)$  representing the minimum time interval between request times of nodes  $n_1$  and  $n_2$ . A node  $n$  contains a set of events from  $ps_{e_i}^M$ . Similar to our handling of events in Section 4.1, four time instances  $earliest[n^r]$ ,  $latest[n^r]$ ,  $earliest[n^f]$ ,  $latest[n^f]$  are defined for each node  $n$  in the preemption chain. The upper and lower bound computation time of a node  $n$  are denoted as  $C^u(n)$  and  $C^l(n)$  respectively; these estimates are obtained from summing up the WCET/BCET of the events in node  $n$ .

The algorithm to construct *preemption chain* is shown in Figure 8, which takes  $ps_{e_i}^M$  as input. Events that may execute concurrently are grouped into one node - the release of any of these events may cause all of them to preempt  $e_i$  in the worst case. Note that such a node is ready when any of its events is ready (see line 4 of the merge procedure in Figure 8). Intuitively, for the WCRT calculation of  $e_i$ , events in a node  $n$  will have the same number of preemptions on the preempted event  $e_i$  in the worst case if their execution interval is not *separated* (as defined in Section 4.1). In our example, suppose  $e2$  executes between time interval  $[3, 6]$ , and  $e3$  executes between  $[4, 7]$ . Then every time  $e2$  preempts  $e1$ , it is also possibly for  $e3$  to preempt  $e1$  before  $e1$  resume its execution. Thus, when considering the worst-case preemption scenario, we can group  $e2$  and  $e3$  into a single node  $n_1$ , which has an earliest ready time of 3, and execution time of  $c_2^u + c_3^u$ . On other hand, suppose  $e4$ 's earliest ready time is 10. In this case,  $e1$  could finish its execution in the interval between  $e2$  and  $e3$  finish execution to  $e4$  gets

```

1 ConstructPC( $ps_{e_i}^M$ ){
2   /*initialize*/
3    $PC = empty$ ; /*the preemption chain*/
4   for(each  $e_j$  in  $ps_{e_i}^M$  as the partial order  $\preceq^M$  of MSC  $M$ ){
5     create a node  $n$  containing  $e_j$ ;
6     /*insert  $n$  into  $PC$ */
7     if( $PC$  is empty)  $PC.insert(n)$ ;
8     else if( $\neg separated(n, source(PC))$ )
9       merge( $n, source(PC)$ ); /*merge  $n$  into  $source(PC)$ */
10    else if( $earliest[n^r] > earliest[source(PC)^r]$ )
11      insertAfter( $n, source(PC)$ ); /*insert  $n$  after  $source(PC)$ */
12    else /* $n$  is ready before  $source(PC)$ */
13      insert  $n$  as the source node of  $PC$ ;
14  }
15  for(each edge  $E(n, n_1)$  in  $PC$ )
16     $W(n, n_1) = earliest[n_1^r] - earliest[n^r]$ ;
17   $W(sink(PC), source(PC)) = P(M) - latest[sink(PC)^r]$ 
18    +  $earliest[source(PC)^r]$ ;
19 }

1 merge( $n, n_1$ ){
2    $C^u(n_1) = C^u(n_1) + C^u(n)$ ; //update computation time
3    $earliest(n_1^r) = \min\{earliest(n_1^r), earliest(n^r)\}$ ;
4    $latest(n_1^r) = \min\{latest(n_1^r), latest(n^r)\}$ ;
5    $earliest(n_1^f) = \max\{earliest(n_1^f), earliest(n^f)\}$ ;
6    $latest(n_1^f) = \max\{latest(n_1^f), latest(n^f)\}$ ;
7 }

1 insertAfter( $n, n_1$ ){
2   if( $succ(n_1)$  not exist)
3     insert  $n$  as the sink node of  $PC$ ;
4   else if ( $\neg separated(n, succ(n_1))$ )
5     merge( $n, succ(n_1)$ );
6   else if( $earliest[n^r] > earliest[succ(n_1)^r]$ )
7     insertAfter( $n, succ(n_1)$ );
8   else
9     insert  $n$  between  $n_1$  and  $succ(n_1)$ ;
10 }

```

$pred(n)/succ(n)$  denote immediate predecessor,  
and successor of  $n$  in the preemption chain.

Figure 8: Constructing a preemption chain.

released. Thus, number of preemptions caused by node  $n_1$  and the node containing  $e_4$  could be different. Finally, such a node is ready when any of its events is ready (see line 4 of `merge` procedure in Figure 8). The distance between two nodes will be the minimum time elapsed between their ready time (line 16 of `constructPC`).

Given the preemption chain  $PC_{e_i}^M$  as defined in the preceding, we need to find the maximum preemption cost it imposes on  $e_i$  during the worst case response time  $w_i$  of  $e_i$ . This is equivalent to the problem of finding the *request bound function* of a recurring real-time task within a time interval  $t$  which is discussed by Baruah in [3]. The **request bound function**,  $PC_{e_i}^M.rbf(t)$ , accepts a non-negative real number  $t$ , and returns the maximum cumulative execution requirement by releasing of nodes in  $PC_{e_i}^M$  that have their ready times within any time interval of duration  $t$ . We will discuss how the request bound can be calculated when we present our analysis for the full-fledged MSG where conditional branches are added.

Given the request bound of  $PC_{e_i}^M.rbf(t)$ , the worst case preemption cost imposed on an event  $e_i$  by the execution of an independent MSC  $M$  within time interval  $t$  (quantity WD in Eq. 3) is

$$WD_i^n = PC_{e_i}^M.rbf(w_i^n)$$

The calculation for the best case preemption cost is similar modulo the following changes:

- Events are grouped into a node of the preemption chain only if they are guaranteed to execute simultaneously, i.e. replace the condition check  $\neg separated(n, n_1)$  by  $concurrent(n, n_1)$  when constructing the *preemption chain*.
- The computation requirement of a node is replaced with the summation of the lower bound computation times.
- The distance between two connected nodes is modified to represent the *maximum* time interval between ready times of the two node.
- The request bound function for  $PC_{e_i}^M.rbf(t)$  is modified to return the minimum cumulative execution requirement.

The best case preemption cost imposed on an event  $e_i$  via execution of other MSC  $M$  (quantity BD in Eq. 4) is

$$BD_i^n = PC_{e_i}^M.rbf(b_i^n)$$

### 4.3 Preemption by MSGs

A MSG modeled application may contain multiple MSC connected by conditional branches, describing its reactions to different environment input (e.g., the packet types obtained as input in an MPEG decoder). To calculate the worst case preemption cost imposed on event  $e_i$  by a complete run of application  $A$ , we first construct a *preemption graph*  $PG_{e_i}^A$  capturing the dependencies between the events in  $A$  that can preempt  $e_i$ 's execution. This is done via the following steps.

1. We construct the preemption chain  $PC_{e_i}^M$  for each MSC  $M$  in  $A$ , based on the algorithm in Figure 8.

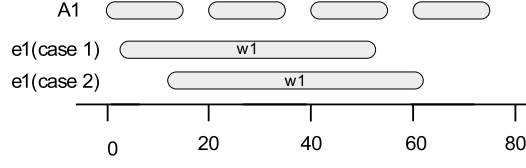


Figure 9: Preemption from Other Applications.

2. If  $M'$  is a successor MSC of  $M$  in the MSG for application  $A$ , we create a directed edge  $E(M, M')$  from  $sink(PC_{e_i}^M)$  to  $source(PC_{e_i}^{M'})$  with weight of

$$earliest[source(PC_{e_i}^{M'})^r] - earliest[sink(PC_{e_i}^M)^r]$$

that is, the minimum distance between ready time of  $sink(PC_{e_i}^{M_i})$  and  $source(PC_{e_i}^{M_j})$ .

3. Finally, we create a unique dummy source node for the preemption graph, denoted as  $source(PG_{e_i}^A)$ , representing the start time of application  $A$ . The dummy node is set as the immediate predecessor of each preemption chain  $PC_{e_i}^M$  which have no predecessor, with the weight of these edges (from the dummy node) being  $earliest[source(PC_{e_i}^M)^r]$ .

The above *preemption graph*  $PG_{e_i}^A$  captures the release information as well as path information of events in application  $A$  that preempt event  $e_i$ . Thus, the WCRT of  $e_i$  can be found by computing the preemption cost from each of such applications over  $e_i$ 's response time. Our *preemption graph* is similar to the graphical representation of a recurring real-time task in [3], where (i) each node is labeled with its execution requirement; (ii) edges are weighted with the minimum triggering-times between two nodes; (iii) two out-going edges from a node represent conditional choice; (iv) and the unique source node is triggered periodically. Thus, our problem of finding  $PG_{e_i}^A.rbf(w_i^n)$ , the maximum cumulative execution requirement by releasing of nodes in  $PG_{e_i}^A$  over  $e_i$ 's  $n$ -th iteration response time  $w_i^n$ , can be converted to the problem of computing the *request bound function* of a recurring real-time task over a given time interval. Note that in recurring real-time tasks, each node also has a deadline. However, this deadline information will not be used when calculating the request bound function. The full-detailed computation for *request bound function* can be found in [3]. In this technical report, we will briefly discuss how the *request bound function* can be calculated given the *preemption graph*.

A MSG modeled application may contain multiple MSC connected by conditional branches, describing its reactions to different environment input (*e.g.*, the packet types obtained as input in an MPEG decoder). Consider an event  $e_1$  of response time  $w_1 = 50$  preempted by events in an application  $A$  with period of 20, as shown in Fig 9. The cost of  $A$ 's preemption on  $e_1$  within  $e_1$ 's response time can be divided into two parts — (a) preemption of  $e_1$  by several complete runs of  $A$ , and (b) preemption of  $e_1$  by possible incomplete runs of  $A$  at the beginning and end of  $e_1$ 's response time. Hence, the number of complete runs of  $A$  within the response time  $w_i$  of  $e_i$  may be either  $\lfloor \frac{w_i}{P} \rfloor - 1$  as shown in case 1 of Figure 9, or  $\lfloor \frac{w_i}{P} \rfloor$  as shown in case 2 of Figure 9.

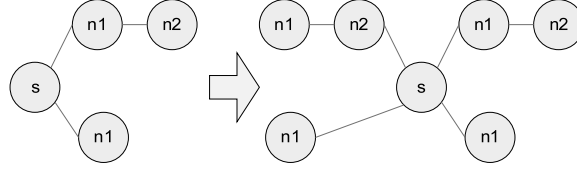


Figure 10: Constructing a super preemption graph.

Clearly, the worst-case preemption cost on  $e_i$  from a complete run of  $A$  — denoted as  $C(PG_{e_i}^A)$  — is the maximum cumulative execution requirement of all nodes along any path in  $PG_{e_i}^A$  from the source node to any of the sink nodes.

Finally, we calculate the preemption cost imposed on an event  $e_i$  from incomplete runs of application  $A$ . As in [?], we construct a super preemption graph  $SPG_{e_i}^A$  by connecting two copies of  $PG_{e_i}^A$ . One edge is added between each sink node ( $n_{sink}$ ) of the first copy and the dummy source node of the second copy, with weight of  $P - latest[n_{sink}^r]$  where  $P$  is the period. Then the dummy source node of the first copy as well as all its outgoing edges are removed from the super graph. Fig 10 shows the super graph construction with an example.

The super graph depicts all possible preemption behaviors for the *two possible incomplete runs of  $A$  at the beginning and end of the response time of  $e_i$* , ignoring the complete runs of  $A$  in between. If the response time  $w_i$  of  $e_i$  is less than the period  $P$  of  $A$ , the *request-critical trace* can be found from all node sequences in  $SPG_{e_i}^A$  (the dummy source node need not be included). However, if  $w_i \geq P$ , the dummy source nodes must be included in the *request-critical trace* for the two incomplete runs of  $A$  within event  $e_i$ 's response time, that is, they must span over two releases of  $A$ . Let us denote the maximum cumulative execution requirement of nodes in  $SPG_{e_i}^A$  over time interval  $t$  to be  $SPG_{e_i}^A.rbf(t)$  if the corresponding *request-critical trace* includes the dummy source node, or  $SPG_{e_i}^A.rbf'(t)$  otherwise. The worst-case preemption cost on  $e_i$  from other applications (the quantity WD in equation 3 can be expressed as follows.

$$WD_i^n = \sum_{A_j} \begin{cases} SPG_{e_i}^A.rbf'(w_i^n), & \text{if } w_i^n < P_j; \\ \max\{\lfloor \frac{w_i^n}{P_j} \rfloor \cdot C(PG_{e_i}^{A_j}) + SPG_{e_i}^{A_j}.rbf(w_i^n \bmod P_j), \\ (\lfloor \frac{w_i^n}{P_j} \rfloor - 1) \cdot C(PG_{e_i}^{A_j}) + \\ SPG_{e_i}^{A_j}.rbf(P_j + w_i^n \bmod P_j)\}, & \text{otherwise.} \end{cases} \quad (5)$$

Similarly, to find the best-case preemption cost, we need to construct the preemption graph and super preemption graph with the weight of edges showing the *maximum* time interval between two connected nodes, and find the minimum cumulative execution requirement over given time interval in the graph. Similar to Equation 5, we obtain:

$$BD_i^n = \sum_{A_j} \begin{cases} SPG_{e_i}^A.rbf'(b_i^n), & \text{if } b_i^n < P_j; \\ \min\{\lfloor \frac{b_i^n}{P_j} \rfloor \cdot C(PG_{e_i}^{A_j}) + SPG_{e_i}^{A_j}.rbf(b_i^n \bmod P_j), \\ (\lfloor \frac{b_i^n}{P_j} \rfloor - 1) \cdot C(PG_{e_i}^{A_j}) + \\ SPG_{e_i}^{A_j}.rbf(P_j + b_i^n \bmod P_j)\}, & \text{otherwise.} \end{cases} \quad (6)$$

## 5 Case Study

### 5.1 Experimental Setup

In this section, we illustrate our analysis method by applying it to a setup from the automotive electronics domain. The system architecture of a FlexRay-based ECU network and two distributed applications (adaptive cruise control, advanced crash preparation) were presented in Section 2.2. The underlying system architecture consists of four ECUs communicating via a shared FlexRay bus, as shown in Figure 1. We assume ECU1 implements a Time Division Multiple Access (TDMA) scheduler, while the remaining three ECUs use preemptive fixed-priority scheduling.

Communication on the FlexRay bus takes place in periodic cycles (or bus cycles), where each cycle is partitioned into a static (ST) and a dynamic (DYN) segment. The ST segment implements a time-triggered protocol, based on the TDMA policy. It is divided into several fixed static slots, and messages can only be sent during their allocated slots. On the other hand, the DYN segment implements an event-triggered bus protocol based on fixed priority scheduling policy. In our analysis, we assume all ST messages sent by tasks mapped on a same ECU to use the same ST slot (*e.g.*,  $m_5$  and  $m_6$  will be transmitted via the same ST slot). Further details of the FlexRay communication protocol can be found in [11] and [20]. Similarly as for events, we also compute the response times for each FlexRay message between its ready time (generated by the sender) and finish time (available to the receiver). For a ST message  $m_i$  with a transmission time of  $C_i$ , we have

$$b_i = C_i; \quad w_i^{n+1} = C_i + T + St(w_i^n) \times T;$$

where  $T$  is the length of the bus communication cycle, and  $St(w_i^n)$  is the number of occurrences of higher priority ST messages using the same ST slot as  $m_i$ , within a time interval of length  $w_i^n$ . For a DYN message  $m_i$ , the response time is calculated as

$$b_i = C_i; \quad w_i^{n+1} = C_i + T + Dyn(w_i^n) \times T;$$

where  $Dyn(w_i^n)$  is the number of occurrences of higher priority DYN messages  $m_j$  within  $w_i^n$  time units, such that  $m_j$  and  $m_i$  are not allowed to be transmitted in the same bus cycle (due to size restriction of the DYN segment). Table 1 outlines the static priorities and computation times for each local computation event and FlexRay message. The best and worst case execution times listed in table 1 correspond to all the four ECUs running at a clock frequency of 500 MHz. The two applications receive data periodically from the external environment (*i.e.* radars and sensors), and are required to complete before the next arrival of their input data (*i.e.* deadlines are equal to periods). We assume input data received by the four radars and the sensor every 100 ms and 50 ms respectively. Thus, period and deadline of the ACC application are 50 ms, and 100 ms for the ACP. Furthermore, we assume the FlexRay bus has a communication cycle of 5 ms.

### 5.2 Results

In this section we present the results obtained by analyzing the setup described above using our proposed analysis technique. Further, we compare these results with those

id	priority	workload(ms)	id	priority	workload(ms)
e1	TDMA	[3,3]	e2	TDMA	[3,3]
e3	2(ECU2)	[3,5]	e4	2(ECU4)	[2,5]
e5	3(ECU2)	[3,4]	e6	1(ECU2)	[1,4]
e7	1(ECU3)	[1,1]	e8	1(ECU4)	[1,2]
e9	2(ECU3)	[2,4]	e10	3(ECU3)	[1,2]
e11	4(ECU3)	[2,2]	e12	TDMA	[3,3]
e13	TDMA	[3,3]	e14	4(ECU2)	[3,6]
e15	3(ECU4)	[2,5]	e16	5(ECU2)	[2,2]
m1	1(st1)	[1,1]	m2	2(st1)	[1,1]
m3	1(DYN)	[1,1]	m4	2(DYN)	[1,1]
m5	1(st3)	[1,1]	m6	2(st3)	[1,1]
m7	1(st2)	[1,1]	m8	1(st4)	[1,1]
m9	3(st1)	[1,1]	m10	4(st1)	[1,1]
m11	3(DYN)	[1,1]	m12	4(DYN)	[1,1]

Table 1: Priorities and workload for the different events/messages shown in Figure 1.

	ACC	ACP
<i>Proposed analysis</i>	48 ms	95 ms
<i>Saksena and Karvelas [23]</i>	60 ms	110 ms

Table 2: End-to-end delay (from sensor/radar to actuator) for the ACC and ACP applications shown in Figure 1.

obtained from standard response time analysis techniques [23] for UML-based system models of multi-threaded implementations of objects/processes, where the dependency between events are not considered. Note that both, our proposed analysis, as well as the one in [23] are *safe*, i.e. if the analysis returns “schedulable” then it is guaranteed to be so.

Table 2 shows the results obtained using the two techniques when all the ECUs run at a clock frequency of 500 MHz. Note that while our analysis returns a “schedulable” result (i.e. the end-to-end delays of the two applications are lower than the sampling periods of the radars/sensors that feed data into them), the analysis proposed in [23] returns “not schedulable”.

Figure 11 shows the estimated end-to-end delays of the ACP application using the two analysis techniques when the clock frequencies of ECU2 and ECU4 are chosen between 400 to 700 MHz at a scale of 100 MHz, with the execution times of the associated tasks being scaled accordingly. The frequencies of the remaining ECUs are kept at 500 MHz. Clearly, the delay estimates obtained using our technique are considerably tighter than those obtained using [23] (12% to 16% improvements). Such tighter estimates immediately translate into better resource dimensioning and system design. In Figure 11 the clock frequencies are scaled in steps of 100 MHz. It may be noted that our analysis returns “not schedulable” only for two different combinations of frequency settings, viz. (ECU2:400 MHz, ECU4: 500 MHz) and (ECU2:400 MHz, ECU4: 400 MHz), from our underlying design space. On the other hand, the analysis proposed in [23] marks a much larger portion of the design space as “not schedulable”. In particular, only (ECU2:700 MHz, ECU4: 600 MHz) and (ECU2:700 MHz, ECU4: 700 MHz), are estimated to be feasible clock frequencies.

There are a number of reasons behind the tighter estimates on the end-to-end delays resulting from our proposed analysis. We discuss some of them below.

- On ECU2:  $e_{16}$  is dependent on  $e_{14}$ . Hence, execution of  $e_{16}$  will never get preempted by  $e_{14}$  in the same iteration of the ACP application.

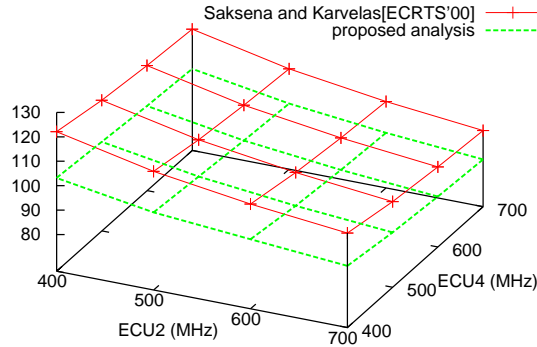


Figure 11: End-to-end delay estimates for the ACP application obtained using our proposed analysis and the technique presented in [23].

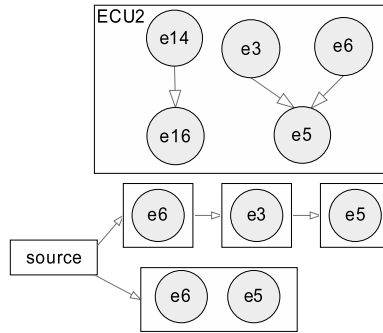


Figure 12: Preemption graph for  $e_{14}$  by events from the ACC application.

- On ECU4: The execution intervals of  $e_4$  and  $e_8$  of the ACC application are not interleaving. It can be guaranteed that one execution of  $e_{15}$  will not be preempted by both  $e_4$  and  $e_8$ .
- On ECU2: The set of events in ACC that can possibly contend with  $e_{14}$  are  $ps_{e_{14}}^{b1} = \{e_6, e_3, e_5\}$  if the MSC  $b1$  in Figure 2(a) is executed; or  $ps_{e_{14}}^{b2} = \{e_6, e_5\}$  if MSC  $b2$  is executed. The dependency information and the resulting *preemption graph* as discussed in Section 4.3 is shown in Figure 12. By computing the request bound function of this preemption graph over the response time of  $e_{14}$ , our analysis estimates that it is not possible for all three events from ACC application ( $e_3$ ,  $e_5$ , and  $e_6$ ) to preempt a single execution of  $e_{14}$ . The worst case actually happens when  $e_3$  preempts  $e_{14}$  first, followed by  $e_5$ , which also holds for the event  $e_{16}$ .

None of the above scenarios can be taken into account in the technique presented in [23] which, as shown above, leads to pessimistic bounds on end-to-end delay estimates.

## 6 Concluding Remarks

In this report, we have presented a schedulability analysis technique for MSG-based modeling of distributed real-time systems. This makes schedulability analysis techniques accessible to formal system specifications such as MSCs which have long been studied in the context of the Unified Modeling Language (UML). We show the utility of our modeling and response-time analysis with real-life applications from the automotive electronics domain. Our experiments show that our method can consider the event dependencies as prescribed by an MSC partial order as well as sequencing and branching between MSCs in a MSG to produce tight response time estimates of MSG-based system models.

While we focus on synchronously concatenated MSCs within a MSG, our proposed analysis framework can be extended to asynchronous concatenation between MSCs, where events across MSCs are synchronized at process-level instead of MSC-level for synchronous concatenation. For synchronous concatenation, we needed to keep the latest / earliest time for start and finish of each MSC, since events in a MSC can be triggered after all events in the predecessor MSC finish. On the other hand, we will need to track the latest / earliest time instances for each process across MSCs if MSCs are concatenated asynchronously.

Another popular mechanism of presenting a collection of MSCs is called high-level MSCs (HMSCs) [15], where MSCs are grouped together in a hierarchical manner. To apply our schedulability analysis to a HMSC-based system model, we could simply flatten the HMSC to an MSG and employ the techniques described in this work. However, such an analysis would not properly exploit the hierarchical structure of the HMSC. This is a topic of our current and future work.

## References

- [1] R. Alur, K. Etessami, and M. Yannakakis. Realizability and verification of MSC graphs. In *ICALP*, 2001.
- [2] R. Alur and M. Yannakakis. Model checking message sequence charts. In *CONCUR*, 1999.
- [3] S. Baruah. Dynamic- and static-priority scheduling of recurring real-time tasks. *Real-Time Systems*, 24(1):93–128, 2003.
- [4] S. Baruah, D. Chen, S. Gorinsky, and A. Mok. Generalized multiframe tasks. *Real-Time Systems*, 17(1):5–22, 1999.
- [5] S. Baruah, R. Howell, and L. Rosier. Algorithms and complexity concerning the preemptive scheduling of periodic, real-time tasks on one processor. *Real-Time Systems*, 2:301–324, 1990.
- [6] A. Burns. *Advances in Real-Time Systems*, chapter Preemptive priority based scheduling: An appropriate engineering approach, pages 225 – 248. Prentice-Hall, 1994.
- [7] G. Buttazzo. *Hard Real-Time Computing Systems: Predictable Scheduling Algorithms and Applications*. Kluwer Academic Publishers, Boston, 1997.
- [8] A. Chakrabarti et al. Verifying quantitative properties using bound functions. In *CHARME*, 2005.
- [9] K. Chatterjee et al. Compositional quantitative reasoning. In *QEST*. IEEE Computer Society, 2006.
- [10] P. Eles, K. Kuchcinski, Z. Peng, A. Doholi, and P. Pop. Scheduling of conditional process graphs for the synthesis of embedded systems. In *DATE*, 1998.
- [11] The flexray communications system specifications, ver 2.1. [www.flexray.com](http://www.flexray.com), 2005.

- [12] R. Gerber, W. Pugh, and M. Saksena. Parametric dispatching of hard real-time tasks. *IEEE transactions on computers*, 44(3):471–479, 1995.
- [13] M. G. Harbour, M. H. Klein, and J. P. Lehoczky. Timing analysis for fixed-priority scheduling of hard real-time systems. *IEEE Transactions on Software Engineering*, 20(1):13 – 28, 1994.
- [14] D. Harel and P. Thiagarajan. *UML for Real: Design of Embedded Real-time Systems*, chapter Message Sequence Charts. Kluwer, 2003.
- [15] ITU-T. 120: Message sequence chart (msc). *ITU-T, Geneva*, 1996.
- [16] J. P. Lehoczky. Fixed priority scheduling of periodic task sets with arbitrary deadlines. In *RTSS*, 1990.
- [17] S. Manolache, P. Eles, and Z. Peng. Schedulability analysis of applications with stochastic task execution times. *ACM Transactions in Embedded Computing Systems (TECS)*, 3(4):706–735, 2004.
- [18] A. Mok and D. Chen. A multiframe model for real-time tasks. *IEEE Transactions on Software Engineering*, 23(10):635–645, 1997.
- [19] P. Pop, P. Eles, and Z. Peng. Schedulability analysis for systems with data and control dependencies. In *ECRTS*, 2000.
- [20] T. Pop, P. Pop, P. Eles, Z. Peng, and A. Andrei. Timing Analysis of the FlexRay Communication Protocol. *ECRTS*, pages 203–213, 2006.
- [21] O. Redell and M. Sanfridson. Exact best-case response time analysis of fixed priority scheduled tasks. In *ECRTS*, 2002.
- [22] M. Reniers. *Message Sequence Chart: Syntax and Semantics*. PhD thesis, Technical University of Eindhoven, Netherlands, 1999.
- [23] M. Saksena and P. Karvelas. Designing for schedulability: Integrating schedulability analysis with object-oriented design. In *ECRTS*, 2000.
- [24] F. Slomka, J. Zant, and L. Lambert. Schedulability analysis of heterogeneous systems for performance message sequence chart. *Proc. Intl Workshop on Hardware/Software Co-Design*, pages 91–95, 1998.
- [25] T. Yen and W. Wolf. Performance Estimation for Real-Time Distributed Embedded Systems. *IEEE Transactions on Parallel and Distributed Systems*, 9(11), 1998.